- Requested start date: February 1st, 2024, requested proposal duration: 5 years

- Related Letter of Intent (LOI): None

- Related preliminary proposal: None

- Prime organization: Whittier College

- Primary place of performance:

  - Organization name: Whittier College
  - Country: United States of America
  - Street address: 3406 E. Philadelphia Street
  - City: Whittier
  - State: California
  - ZIP Code: 90602

- Other federal agencies: None

- Other information: Antarctic fieldwork

NSF-CAREER: Translation of Machine Learning and Additive Manufacturing to Accelerate and Diversify Science and Engineering

Radio-frequency (RF) phased-array systems optimized with machine learning have become powerful tools in science and engineering. Recent progress in phased-array radar development has applications in particle astrophysics [1–4], polar research [5,6], and 5G mobile communications [7]. Phased-arrays are comprised of RF antennas working in tandem to boost received signal sensitivity, and to actively scan transmitted signals without moving parts. There are at least two barriers that impede phased-arrays from enhancing future science and engineering projects on a wide scale. First, the computational electromagnetism (CEM) properties of RF systems are designed with expensive, proprietary software that does not interface with open-source machine learning tools [8]. Second, RF systems are manufactured using costly and time-consuming traditional machining techniques. Ongoing scientific and engineering efforts can be enhanced by a solution that allows machine learning optimzation to flourish, reduces design and manufacturing costs, and diversifies participation by reducing financial barriers. Undergraduate education at Whittier College will be enhanced with CEM, machine learning, and 3D printing, as research and educational opportunities will be integrated into the curriculum.

We propose to create the first open-source CEM and additive manufacturing ecosystem capable of 3D-printing phased arrays with conductive filament [8–10]. We have already shown that open-source CEM tools used in photonics can drive the RF phased-array design process [3,11,12]. This research will support diverse projects like IceCube Gen2 (radio), Center for Remote Sensing and Systems (CReSIS) missions, and Office of Naval Research (ONR) radar projects. One application in particle astrophysics is the Askaryan Radio Array (ARA), in which phased arrays have increased sensitivity to ultra high-energy neutrino (UHE-ν) interactions in the ice sheet beneath the South Pole [13]. The arrays are vertically polarized, due to mechanical constraints within the ice. Our research could provide a *horizontally polarized* design that overcomes the mechanical constraints through machine learning, boosting the chances of making the first UHE-ν observations in history [14]. This research will *accelerate* and *diversify* research in UHE-ν, climate science, and RF engineering by *translating* successes in CEM and materials research. This work will be integrated into our curriculum and research programming at Whittier College, a Title-V Hispanic Serving Institution (HSI).

This work will provide research and educational opportunities to diverse undergraduates at Whittier College. We have a proud tradition of providing access to higher education to Spanish-speaking and historically marginalized students, and we are a the only HSI member of the IceCube Gen2 collaboration. People of color and first-generation students make up 63% and 29% of our student body, respectively. Internal assessment studies indicate that students of color receive lower grades than their peers in introductory STEM courses. We have learned from workshops hosted by the Cottrell Scholars Network that emphasizing the dignity and self-efficacy of diverse students can increase their performance [15,16]. Emphasis in these areas makes students feel they *belong* in our courses, despite encountering adversity. In keeping with the theme of *translation*, and in order to emphasize the dignity of our students no matter their background, we seek to create a bilingual (Spanish and English) mobile application (app) that introduces STEM concepts within a welcoming digital environment.

There is precedent for learning apps enhanced by machine learning in the DuoLingo method for language and mathematics [17]. We seek to provide data insights about student learning to instructors through the app, which will lead to more efficient and customized classroom instruction. A prototype application is being built by Whittier College undergraduates. The creation and implementation of this program represents an opportunity for Whittier College students to enhance the learning experience for their peers while gaining valuable coding and machine learning experience. In addition to algorithms presented within the Duolingo method, the educational data mining (EDM) literature provides examples of apps that boost engagement and success in introductory STEM courses [18–21]. Members of our community have shared that translating mathematics and physics exercises into Spanish aids in solving them. Our application will boost their skills and build confidence by offering them engaging, game-like physics training in the language of their choice. Finally, we propose to create a bilingual lecture series and recruitment events designed to welcome the broader community into the Whittier College environment.

Translation of Machine Learning and Additive Manufacturing to Accelerate and Diversify Science and Engineering

Jordan C Hanson, PhD
Assistant Professor of Physics and Astronomy
Whittier College
Whittier, CA

May 29, 2023

Contents

Project Description: Intellectual Merits

Radio-frequency (RF) phased arrays have applications in radar telemetry, telecommunications, ground-penetrating radar, scientific instrumentation, and remote sensing [1,2,5,13,22–24]. In the one-dimensional case, N three-dimensional RF antennas are arranged in a line with fixed spacing. In the two-dimensional case, $N \times M$ three-dimensional antenna elements are arranged in a two-dimensional grid with fixed spacing in both dimensions. The signal to noise ratio (SNR) of received signals in arrays of dimension N is boosted by a factor of $\approx \sqrt{N}$, because the N signals are combined coherently while thermal noise adds like $\sqrt{N}$. The SNR boost is critical for certain kinds of scientific observations. For example, systems created at the Center for Remote Sensing and Integrated Systems (CReSIS) are flown in polar regions to perform radar sounding of ice sheets for the purposes of geophysics and climate science [5]. Reflected signals carry information about the ice depth, temperature, and internal structure of the ice. The radio echoes have small SNR values that require phased arrays.

Traditionally, RF phased arrays are designed with commerical computational electromagnetism (CEM) software. Radio antennas and phased arrays have *radiation patterns* that define directions of maximum transmission power and received sensitivity. Radiation patterns have a main lobe in which most of the radiation is concentrated, and the angular width of the main lobe is called the beam width. Other parameters like S-parameters quantify the efficiency of the systems. CEM packages like XFDTD and HFSS are used to model these properties as a function of frequency [25,26]. The XFDTD package, for example, relies on the finite difference time domain (FDTD) method. The FDTD approach is a CEM technique in which spacetime and Maxwell's equations are broken into discrete form. HFSS uses a similar approach in the Fourier domain, the Finite Element Method (FEM). Depending on the software license and version, the current price of these products ranges between $5,000 and $40,000 USD. These costs are prohibitive for HSI undergraduate institutions like Whittier College. Removing this financial barrier to entry would enable diverse researchers to gain important skills in the field of RF design.

Another drawback of commercial CEM software is the lack of access to the source code, which impedes the incorporation of modern machine learning packages. Phased array properties are determined by the shape of the RF elements and the grid properties of the array, and the parameter space is driven by the complex variety of RF element shapes. When combined with open-source CEM software, modern machine learning algorithms can locate optimal solutions within the parameter space. The authors of [8] review a number of open-source CEM packages, and conclude that there are viable open-source options for simple RF antenna shapes. For our proposed work, the open-source CEM software must be able to handle the growing complexity of RF antenna designs. One interesting choice is the MIT Electromagnetic Equation Propagation (MEEP) package [12]. Though MEEP was designed for μm wavelengths in photonics applications, we have shown that the scale-invariance of Maxwell's equations allows MEEP users to translate designs to wavelengths at the cm-scale. We have also shown that MEEP can drive the RF phased-array design loop, and that 3D printer schematics can be extracted from this process [3,11,12]. This research represents an opportunity for diverse undergraduates to gain experience applying machine learning tools to the design of practical systems.

Recent advances in materials research have led to the creation of 3D printer filament that has conductivity in RF bands. Funded through an NSF Translational Impact (TI) award (1721644), Multi3D LLC. has
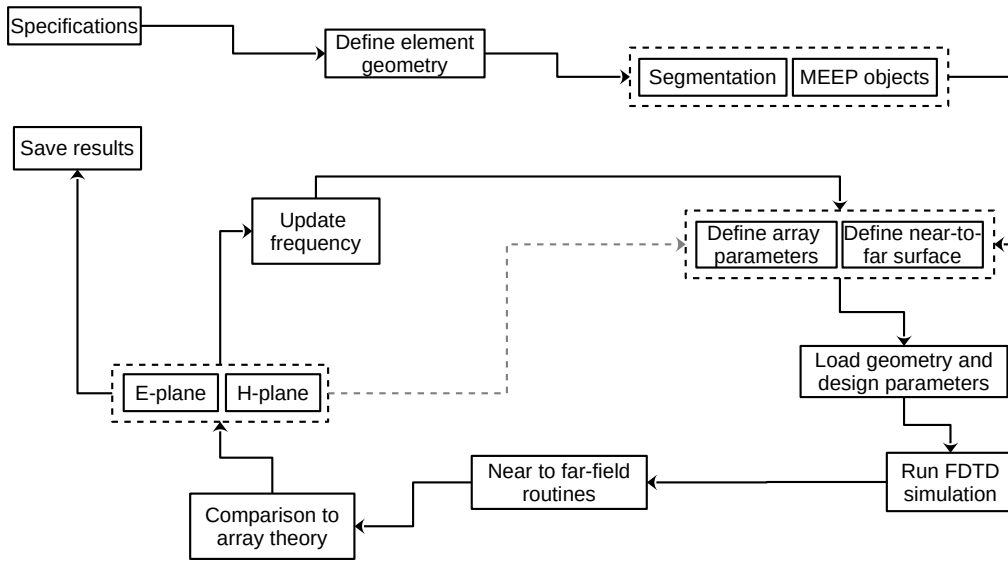
Figure 1.1: Our design process for RF phased arrays from [3], adapted from Fig. 1 of the review [8].

produced filament with a resistivity of just $10^{-2}\Omega$ cm: the Electrifi filament. Several antenna designs have already been produced [10,27]. These examples include horn antennas with gain factors of 15 dB at 5.8 GHz, and microstrip patch antennas with gains of 1-2 dB at 2.5 GHz. The results match expectations from HFSS models, exhibiting no major differences with antennas made using perfect conductors. There are, however, virtually no examples of 3D printed RF phased arrays in the [0.1 - 1] GHz bandwidth. This bandwidth is the most relevant for the aforementioned applications in particle astrophysics and geophysics. Further, whole new designs can be discovered that improve on designs like the horn and patch antennas by merging machine learning packages with MEEP. In Sec. 1.1, we review progress already made at Whittier College. In Sec. 1.2, we show how this work enhances the field of UHE-ν observations. In Sec. 1.3, we show how this work enhances the field of radio echo sounding of ice sheets and ice shelves. In Sec. 1.4, we articulate our vision for the integration of this research into our STEM curriculum at Whittier College. In Sec. 1.5, we make the case that the overall intellectual merits of the proposed activities are sound.

1.1 Computational Electromagnetism and Additive Manufacturing

In Summer 2020, we received a Faculty Fellowship from the Office of Naval Research (ONR) to study and design phased arrays in the [0.1 - 5] GHz bandwidth. This bandwidth is relevant for projects like IceCube Gen2 (radio), and Whittier College is a member institution of the IceCube Gen2 collaboration. With our background in NSF-funded projects like the Antarctic Ross Ice Shelf Antenna Neutrino Array (ARIANNA), the Askaryan Radio Array (ARA), and NASA-funded projects like the Antarctic Impulsive Transient Antenna (ANITA), we were qualified to teach our ONR colleagues about phased array applications. Our goal was to design a phased array system to be integrated as a transmitter in an anechoic chamber. The anechoic chamber will serve as a testing facility for active radar systems. We began by giving lectures on the electromagnetism of phased arrays and scientific and engineering applications. The audience included engineers and programmers that work in acquisition and development for the Naval Surface Warfare Center (NSWC), Corona Division (NSWC Corona). Our design flow is depicted in Fig. 1.1. To minimize costs and increase access to Whittier College students, we decided to investigate open-source CEM options for the design.
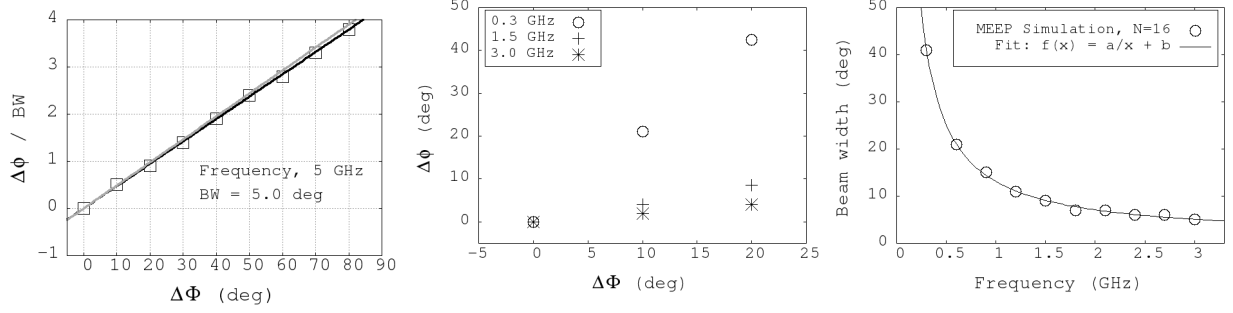
Figure 1.2: (Left) The beam angle $\Delta\phi$ divided by the beam width BW for the $N = 16$ one-dimensional Yagi array versus $\Delta\Phi$, the phase shift per element. The gray line represents theoretical expectation, and the black line is a linear fit to the data. (Middle) $\Delta\phi$ versus $\Delta\Phi$ for the $N = 16$ version of the one-dimensional horn array, for several frequencies. (Right) The dependence of the beam width on frequency for the one-dimensional $N = 16$ horn array. The black line is a functional fit to the data $f(x) = a/x + b$ with $a = 12.0 \pm 0.1$ degree GHz, and $b = 1.1 \pm 0.2$ degrees.

We encountered the aforementioned review article in the open-access journal *Electronics* that indicated there are open-source CEM tools that can be adapted to phased array analysis. Our design flow in Fig. 1.1 is adapted from Fig. 1 of the review to include specific tasks required for phased arrays, and algorithms for the computation of far-field radiation patterns. MEEP was noted by the authors in the review as the most advanced among open-source FDTD programs, but they did not benchmark it against HFSS or XFDTD due to the "steep" learning curve. As part of the ONR Summer Faculty Fellowship, we ascended the learning curve and adapted MEEP to RF systems. The key insight was that MEEP takes advantage of the *scale invariance* of Maxwell's Equations. The simplest way to understand this is to understand how MEEP uses relative units when discretizing Maxwell's equations for Python code.

Like other FDTD CEM methods, MEEP uses a Yee lattice to discretize Maxwell's equations [28]. When the speed of light is set to unity ($c = 1$), distance and time units are set to be the same. Frequency and wavelength units are the inverse of each other. But distance and wavelength can take *any* unit of length in the Yee lattice. Most MEEP users interpret this unit of length to be 1 μm because the applications are for photonics. For example, a *relative* frequency (unit-less) of 0.5 corresponds to a *relative* wavelength of 2. When interpreted as 2 μm, the frequency is 150 THz in real units that correspond to optical bandwidth. If we choose to interpret the *relative* wavelength as 2 cm, the real frequency is 15 GHz. A *relative* frequency of 0.05 corresponds to the RF frequency 1.5 GHz. Assuming design components have sufficient conductivity at RF frequencies, we have re-purposed MEEP as an RF simulator.

By Fall 2020, we were producing CEM models using MEEP that matched expected phased array properties. For a one-dimensional array with N elements, there is a linear relationship between the radiated plane-wave direction $\Delta\phi$, and the phase shift per element $\Delta\Phi$. The coefficient of the relationship is determined by the ratio of real wavelength to element spacing. Figure 1.2 contains results for our first phased array models in which the elements were Yagi-Uda style antennas and horn antennas. The linear relationship is evident in the data. The radiated signal direction $\Delta\phi$ is divided by the beam width (BW) in Fig. 1.2 (left), and is left in degrees in Fig. 1.2 (middle). A beam width of a radiation pattern is the angular width of the main lobe, outside of which the radiated power has decreased by 3 dB. In Fig. 1.2 (left), the $N = 16$ Yagi array can steer a 5 GHz plane wave up to four beam widths to the right or left of the forward direction. Yagi-Uda style antennas are designed for a single frequency. In Fig. 1.2 (middle), results are shown for an $N = 16$ array of horn antennas. Since horn antennas are broadband radiators, the linear relationship is shown for 0.3, 1.5, and 3.0 GHz. The beam width is inversely related to frequency, so $\Delta\phi$ was left in degrees. In Fig. 1.2 (right), the inverse relationship is shown.

We can also produce phased array radiation patterns with MEEP that match theoretical expectations. The radiation pattern of a one-dimensional array of N radiating point sources can be derived using first principles [3]. The *pattern multiplication theorem* states that the radiation pattern of a one-dimensional
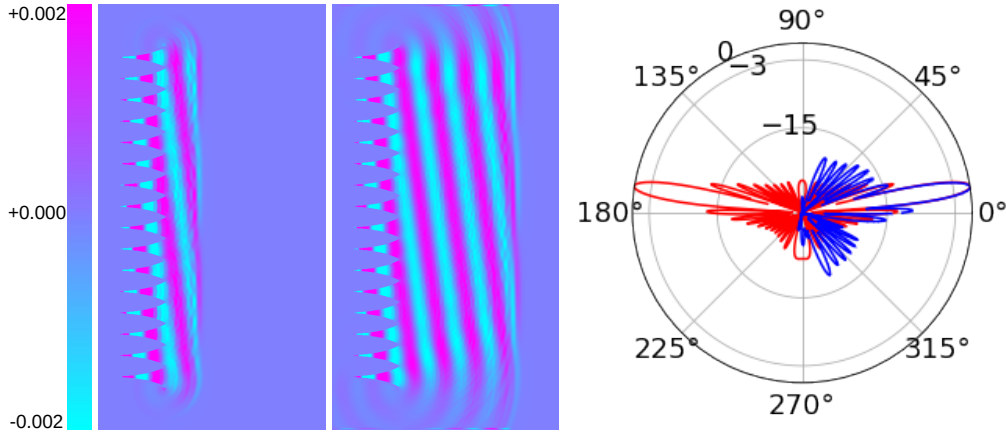
Figure 1.3: (Left) The $N = 16$ one-dimensional horn array, radiating a linearly polarized electric field $\vec{E}(x, y, t)$ (y-component shown, in arbitrary units) at $t = 1$ ns into the simulation run, and (middle) at $t = 2$ ns into the run. The 2D area is 80×150 cm^2. The frequency is 2.5 GHz, and the beam angle is $\Delta\phi = 9$ degrees from broadside (x-direction). (Right) The normalized radiated power in dB versus $\Delta\phi$. The blue curve represents the results from MEEP, and the red curve is the theoretical expectation from N point sources.

phased array of N identical elements will be that of a row of N point sources, multiplied by the radiation pattern of the individual element. In Fig. 1.3 (left and middle), the radiated field of a $N = 16$ horn array is shown in the E-plane (x-y plane). The radiation pattern is shown in 1.3 (right). The main lobe is steered 9 degrees above the x-axis, matching the theoretical expectation. The blue curve in the polar plot represents the CEM radiation pattern from MEEP, while the red curve is the theoretical expectation from a row of N point sources. The row of point sources is symmetric, creating a back lobe at $\Delta\phi = 171$ degrees. The horn array has no back lobe because the individual horns suppress backward radiation, as expected from the pattern multiplication theorem. We also showed that two-dimensional arrays of Yagi-Uda and horn antennas matched theoretical expectations exactly. Our revelation that the photonics code MEEP could used to design phased arrays design earned the final article Top 10 honors for December 2020 to May 2021 from the editors of *Electronics*.

It is important to note that our undergraduate physics, computer science, and engineering curriculum is greatly enhanced by researching applications of CEM. One straightforward example is to incorporate CEM tools like MEEP into lower and upper division electromagnetism and Python3 courses. Our 3-2 Engineering Program students, Physics majors, and Integrated Computer Science (ICS) majors all stand to benefit from learning to use Python to perform computational physics. Our current curriculum does not yet include CEM in lower or upper-division electromagnetism courses, nor is it included in computational physics. Integrating results from this research into course management systems, via MEEP Jupyter notebooks, is a straightforward way to enhance STEM education for our diverse undergraduates. Showcasing the 3D printed RF systems should engage their curiosity by providing a real-world application of course concepts. Finally, given the diverse demographics of our students, enriching their educational experience with real-world applications serves to diversify the STEM workforce. We propose to develop project-based learning (PBL) modules that incorporate RF design, machine-learning, and additive manufacturing for our Whittier College STEM students.

In Summer 2021, we again received a Faculty Fellowship from the ONR to continue this work. We focused on creating realistic 3D models of horn antennas that could be printed with 3D printers. Working with undergraduate researchers, we learned to create designs that can be expressed as Python3 functions and converted to a GDSII CAD file. GDSII files can be imported into MEEP, and converted to STL files for use with a 3D printer. Our CEM codes are therefore using the precise shape that we intend to print. We acquired NinjaTek proto-pasta 3D printer filament, advertised as conductive. We printed a horn with in-built SMA connecter for RF cables (Fig. 1.4). The proto-pasta result had the right shape, but a measured
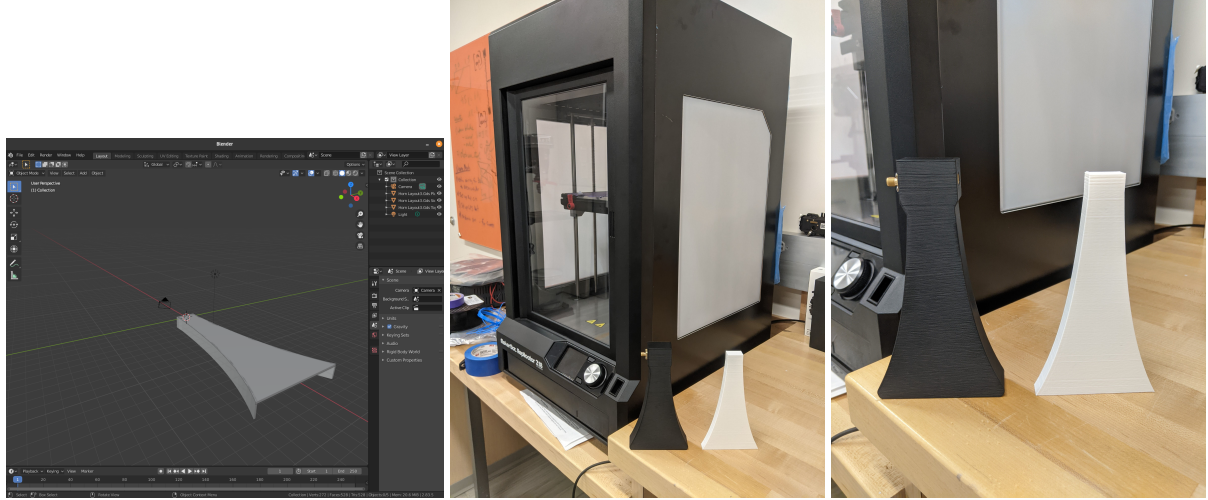
Figure 1.4: (Left) Blender/STL files extracted from MEEP code. (Middle) MakerBot 3D printer, with PLA horn model (white), and proto-pasta with SMA connector (black). (Right) Close-up of horns.

resistance too large for an RF antenna. Multi3D LLC, the manufacturer of the Electrifi filament, has now provided resistivity results that compare proto-pasta with Electrifi (Fig. 1.5). The Electrifi filament will improve resistivity by two orders of magnitude. We seek to print Electrifi-based antennas, and to measure the radiation pattern and S-parameters.

In Summer 2022, we received a final ONR Faculty Fellowship that focused on GPS M-code and modernization. Alongside this work, we continued to refine the open-source RF horns. This included computing radiation patterns and S-parameters for the full 3D horns stored in CAD files. In Fig. 1.6 (a), the main lobes are designed to point to 0 degrees (x-direction) for the E-plane (x-y plane), and 90 degrees for the H-plane (x-z plane). The E-plane is the plane containing the linearly polarized radiation vector, and the H-plane is orthogonal to the E-plane. In Fig. 1.6, the (voltage standing wave ratio) VSWR is shown. The VSWR is a common figure of merit for RF antennas, related to the S11 scattering parameter. The VSWR approaches 1 for an efficiently radiating antenna. The radiation patterns match expectations for horn antennas (see Fig. 19 of [10]). The VSWR results demonstrate efficient radiation in the bandwidth [0.5 - 6] GHz. We presented our progress at the annual MeepCon 2022 at the Massachusetts Institute of Technology (MIT) [11]. We learned the extent to which MEEP can be integrated with Python3-based machine learning tools [29], and how eager MEEP developers are to collaborate in the RF regime. Extending MEEP to RF users widens the user base of MEEP, which has traditionally focused on photonics applications.

Horizontal Traces	Dimension (X × Y × Z cm^3)	Resistance (Ω)	Resistivity (Ω cm)
Electrifi	0.2 × 10 × 0.2	3.0	0.012
Black Magic 3D	0.2 × 10 × 0.2	142.5	0.57
Proto-Pasta	0.2 × 10 × 0.2	1506	6.02

Vertical Towers	Dimension (X × Y × Z cm^3)	Resistance (Ω)	Resistivity (Ω cm)
Electrifi	0.5 × 0.5 × 10	3.4	0.085
Black Magic 3D	0.5 × 0.5 × 10	103.6	2.59
Proto-Pasta	0.5 × 0.5 × 10	410	10.25

Figure 1.5: Resistivity results published by Multi3D LLC that compare the proto-pasta product with the new Electrifi conductive filament (https://www.multi3dllc.com/faqs/).
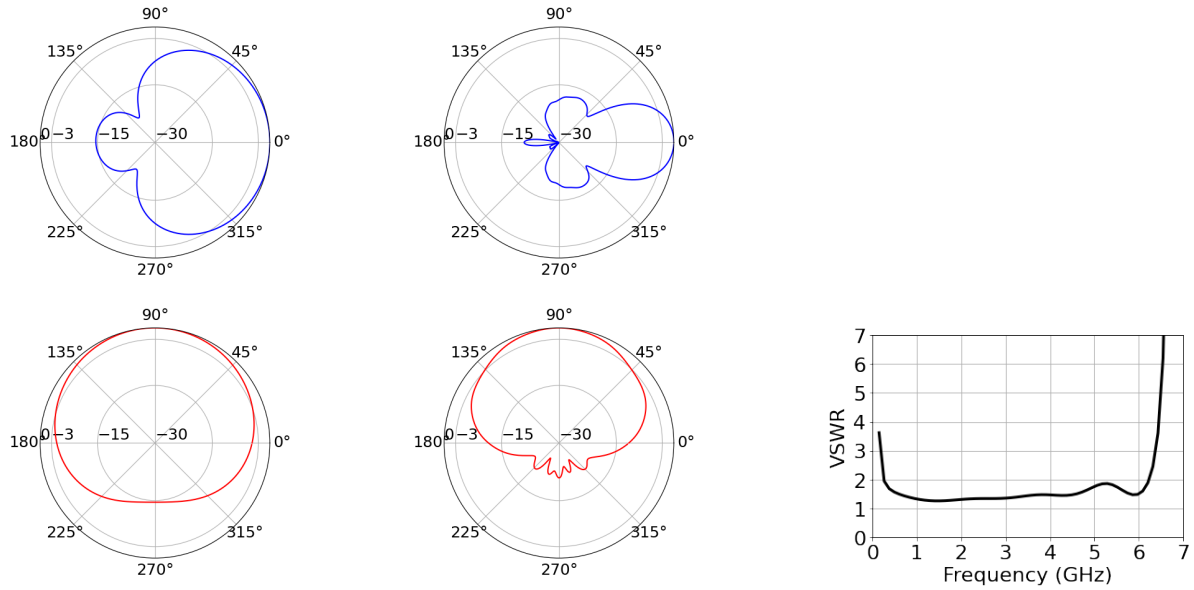
(a) Radiation pattern results using GDSII/CAD for (top left) E-plane at 0.5 GHz, (top right) E-plane at 5.0 GHz, (bottom left) H-plane at 0.5 GHz, (bottom right) H-plane at 5.0 GHz. See text for details.

(b) The VSWR figure of merit versus frequency in GHz for the RF horn.

Figure 1.6: Results for RF horn design, using the open-source design process open to 3D printing.

Student/Professor	Grant Opportunity	Amount	Dates
Jordan C. Hanson	ONR Summer Faculty Fellow	$16.5k	Summer 2022
Raymond Hartig	Ondrasik-Groce Fellowship	$5k	Summer 2022
Jordan C. Hanson	ONR Summer Faculty Fellow	$16.5k	Summer 2021
Adam Wildanger	Fletcher Jones Fellowship	$5k	Summer 2021
Jordan C. Hanson	ONR Summer Faculty Fellow	$16.5k	Summer 2020
Raymond Hartig	Fletcher Jones Fellowship	$5k	Summer 2020
John Paul Gómez-Reed	Ondrasik-Groce Fellowship	$7.5k	Summer-Fall 2019
John Paul Gómez-Reed	Keck Fellowship	$5k	Summer 2018
Cassady Smith	Keck Fellowship	$5k	Summer 2018

Table 1.1: A listing of the grant opportunities awarded to my students and I.

1.1.1 RF Laboratory Capability

According to ONR protocols, I become eligible for Senior Faculty Fellowships once I have been awarded an SFRP Fellowship three times. I am eligible to apply in Summer 2023 after a mandatory one-year cooling period. I have included all funding I have received from the ONR, and all student fellowships that I have received up to the present in Tab. 1.1. I have included all equipment NSWC Corona has donated to Whittier College in Tab. 1.2. These items were at first on loan to us, but are now being converted to donations. There are further HPC resources in preparation to be donated to us, pending approval by senior personnel at the lab. Equipment such as the items in Tab. 1.2 are typically donated to colleges and universities when their project life-cylce is complete at the Navy lab and are no longer necessary. In Sec. **??** below, I articulate a vision for the use of these instruments in Whittier College engineering projects.

Equipment	Purpose	Bandwidth	Cost
Rohde and Schwartz ZVL6 Network Analyzer	Measuring RF power and frequency	9 kHz to 6 GHz	$20k
Rohde and Schwartz NRP-91 Power Sensors (2)	Measuring RF power	9 kHz to 6 GHz	$8k
Aeroflex 3416 Digital RF Signal Generator	Creating RF signals	250kHz to 6 GHz	$12k
Calibration antenna kits (2)	Receiving and transmitting	Varies by antenna	$2k
Calibration test kits for Network Analyzer (2)	Network Analyzer Calibration	6 kHz to 9 GHz	$6k

Table 1.2: A listing of the equipment provided to our labs by the Office of Naval Research.

1.2 The Connection to Ultra-high Energy Neutrino Observations

We have also shown that MEEP can be used to model the behavior of phased arrays in realistic polar ice environments [3, 11, 12]. Most commercial CEM packages assume a uniform ground plane and index of refraction in the medium surrounding the array. By contrast, MEEP gives the user fine control of the index of refraction of each voxel, $n(x, y, z)$. The RF index of refraction in polar ice is $n = 1.78$ for solid ice, but varies with the depth (z) near the snow surface. The transitional region between surface snow and solid ice in polar regions is known as the *firn*. The $n(z)$ function is well-measured in a variety of locations in Antarctica [30], and Greenland [31]. The ARA (South Pole) [13], Radio Neutrino Observatory, Greenland (RNO-G) [32], and the proposed IceCube Gen2 project (South Pole) [33] all use or plan to use RF phased arrays as the primary UHE-ν detector. We propose to incorporate the actual index of refraction profile $n(z)$ into the phased array design process, which is difficult to accomplish with commerical tools.

The common simulation package used for ARA, RNO-G, and IceCube Gen2 is NuRadioMC, built from prior experience with ARA and ARIANNA [34–38]. NuRadioMC addresses analytically the ray-tracing solution for UHE-ν signals as they propagate through polar ice. We derived the analytic ray-tracing solutions presented in [30] and [34], which were adopted into NuRadioMC. The ray-tracing approach is an approximation that does not capture the precise behavior of three-dimensional field propagation in ice with realistic properties. A byproduct of our proposed research will be to incorporate realistic field propagation into NuRadioMC using FDTD computations. This integration should increase the precision of the predictions made by NuRadioMC that will be checked against future ARA, RNO-G, and IceCube Gen2 data for UHE-ν interactions in polar ice volumes [39]. The software development necessary to incorporate FDTD calculations into NuRadioMC also represents a learning opportunity for Whittier College physics and computer science students.

1.3 The Connection to Remote Sensing of Ice Sheets

Example

1.4 Integration of the Research into Educational Programming at Whittier College

Example

1.5 Conclusion, Intellectual Merits

Example

Project Description: Broader Impacts

Overaching Introduction

2.1 Translation of Scientific and Engineering Research

Do people really know how multi-lingual this area is, and why that is important? Cite the creation of *History of Science in Latin America*.

2.2 Mobile Application Development

Educational Application for Systematic Training and Learning of STEM (EASTLOS)

2.3 Bilingual Public Lectures and Recruitment Events

Example

Bibliography

[1] A. Vieregg, K. Bechtol, and A. Romero-Wolf, "A technique for detection of pev neutrinos using a phased radio array," *Journal of Cosmology and Astroparticle Physics*, vol. 2016, p. 005, feb 2016.

[2] J. Avva, K. Bechtol, T. Chesebro, L. Cremonesi, C. Deaconu, A. Gupta, A. Ludwig, W. Messino, C. Miki, R. Nichol, E. Oberla, M. Ransom, A. Romero-Wolf, D. Saltzberg, C. Schlupf, N. Shipp, G. Varner, A. Vieregg, and S. Wissel, "Development toward a ground-based interferometric phased array for radio detection of high energy neutrinos," *Nuclear Instruments and Methods in Physics Research Section A: Accelerators, Spectrometers, Detectors and Associated Equipment*, vol. 869, pp. 46–55, 2017.

[3] J. C. Hanson, "Broadband rf phased array design with meep: Comparisons to array theory in two and three dimensions," *Electronics*, vol. 10, no. 4, 2021.

[4] J. Aguilar, P. Allison, J. Beatty, H. Bernhoff, D. Besson, N. Bingefors, O. Botner, S. Buitink, K. Carter, B. Clark, A. Connolly, P. Dasgupta, S. de Kockere, K. de Vries, C. Deaconu, M. DuVernois, N. Feigl, D. García-Fernández, C. Glaser, A. Hallgren, S. Hallmann, J. Hanson, B. Hendricks, B. Hokanson-Fasig, C. Hornhuber, K. Hughes, A. Karle, J. Kelley, S. Klein, R. Krebs, R. Lahmann, M. Magnuson, T. Meures, Z. Meyers, A. Nelles, A. Novikov, E. Oberla, B. Oeyen, H. Pandya, I. Plaisier, L. Pyras, D. Ryckbosch, O. Scholten, D. Seckel, D. Smith, D. Southall, J. Torres, S. Toscano, D. V. D. Broeck, N. van Eijndhoven, A. Vieregg, C. Welling, S. Wissel, R. Young, and A. Zink, "Design and sensitivity of the radio neutrino observatory in greenland (RNO-g)," *Journal of Instrumentation*, vol. 16, p. P03025, mar 2021.

[5] E. Arnold, C. Leuschen, F. Rodriguez-Morales, J. Li, J. Paden, R. Hale, and S. Keshmiri, "Cresis airborne radars and platforms for ice and snow sounding," *Annals of Glaciology*, vol. 61, no. 81, p. 58–67, 2020.

[6] L. Li, J.-B. Yan, C. O'Neill, C. D. Simpson, and S. P. Gogineni, "Coplanar side-fed tightly coupled ultra-wideband array for polar ice sounding," *IEEE Transactions on Antennas and Propagation*, vol. 70, no. 6, pp. 4331–4341, 2022.

[7] S. Hussain, S.-W. Qu, A. Sharif, H. Abubakar, X.-H. Wang, M. Imran, and Q. Abbasi, "Current sheet antenna array and 5g: Challenges, recent trends, developments, and future directions," *Sensors*, vol. 22, no. 9, 2022.

[8] A. Fedeli, C. Montecucco, and G. L. Gragnani, "Open-Source Software for Electromagnetic Scattering Simulation: The Case of Antenna Design," *Electronics*, vol. 8, no. 12, p. 1506, 2019.

[9] O. Yurduseven, S. Ye, T. Fromenteze, B. Wiley, and D. Smith, "3d conductive polymer printed metasurface antenna for fresnel focusing," *Designs*, vol. 3, no. 46, 2019.

[10] F. Pizarro, R. Salazar, E. Rajo-Iglesias, M. Rodríguez, S. Fingerhuth, and G. Hermosilla, "Parametric study of 3d additive printing parameters using conductive filaments on microwave topologies," *IEEE Access*, vol. 7, pp. 106814–106823, 2019.

[11] J. Hanson, "Broadband rf phased array design with meep." MeepCon 2022, 2022.

[12] A. F. Oskooi, D. Roundy, M. Ibanescu, P. Bermel, J. Joannopoulos, and S. G. Johnson, "Meep: A flexible free-software package for electromagnetic simulations by the FDTD method," *Computer Physics Communications*, vol. 181, no. 3, pp. 687–702, 2010.

[13] P. Allison and et al, "Low-threshold ultrahigh-energy neutrino search with the askaryan radio array," *Phys. Rev. D*, vol. 105, p. 122006, Jun 2022.

[14] Anker, A, et al, "Probing the angular and polarization reconstruction of the ARIANNA detector at the South Pole," *Journal of Instrumentation*, vol. 15, no. 09, pp. P09039–P09039, 2020.

[15] M. Estrada, "Creating pathways of kindness and inclusion in stem education." Inclusivity in Introductory STEM Courses, 2022.

[16] C. Singh, "Promoting equity in science learning." Inclusivity in Introductory STEM Courses, 2022.

[17] C. Freeman, A. Kittredge, H. Wilson, and B. Pajak, "The duolingo method for app-based teaching and learning," tech. rep., Duolingo Research Report, 2023.

[18] D. Shin and J. Shim, "A systematic review on data mining for mathematics and science education," *International Journal of Science and Mathematics Education*, pp. 1–21, 2020.

[19] C. Cooper and P. Pearson, "A genetically optimized predictive system for success in general chemistry using a diagnostic algebra test," *Journal of Science Education and Technology*, vol. 21, no. 1, 2011.

[20] J. Grossman, Z. Lin, H. Sheng, J. Wei, J. Williams, and S. Goel, "Mathbot: Transforming online resources for learning math into conversational interactions," *Association for the Advancement of Artificial Intelligence (www.aaai.org)*, 2019.

[21] H. Lee and "et al", "Automated text scoring and real-time adjustable feedback: Supporting revision of scientific arguments involving uncertainty," *Science Education Journal*, vol. 103, no. 3, 2019.

[22] J. Ghimire, F. D. Diba, J.-H. Kim, and D.-Y. Choi, "Vivaldi Antenna Arrays Feed by Frequency-Independent Phase Shifter for High Directivity and Gain Used in Microwave Sensing and Communication Applications.," *Sensors (Basel, Switzerland)*, vol. 21, no. 18, p. 6091, 2021.

[23] F. Cui, G. Dong, Y. Chen, C. Wang, D. Teng, and R. Wang, "Numerical modeling and data signal analysis of GPR array based on dual-field domain-decomposition time-domain finite element method," *Journal of Applied Geophysics*, vol. 208, p. 104876, 2023.

[24] R. Mailloux, *The Phased Array Handbook, 3rd ed.* Boston: Artech House, 2017.

[25] "Xfdtd 3d electromagnetic simulation software." https://www.remcom.com. Accessed: 2023-05-23.

[26] "Ansys hfss." https://www.ansys.com. Accessed: 2023-05-23.

[27] O. Yurduseven, P. Flowers, S. Ye, D. L. Marks, J. N. Gollub, T. Fromenteze, B. J. Wiley, and D. R. Smith, "Computational microwave imaging using 3D printed conductive polymer frequency-diverse metasurface antennas," *IET Microwaves, Antennas & Propagation*, vol. 11, no. 14, pp. 1962–1969, 2017.

[28] K. Yee, "Numerical solution of initial boundary value problems involving maxwell's equations in isotropic media," *IEEE Transactions on Antennas and Propagation*, vol. 14, no. 3, pp. 302–307, 1966.

[29] A. Hammond, "High-performance topology optimization for photonics inverse design." MeepCon 2022, 2022.

[30] S. Barwick, E. Berg, D. Besson, G. Gaswint, C. Glaser, A. Hallgren, J. Hanson, S. Klein, S. Kleinfelder, L. Köpke, I. Kravchenko, R. Lahmann, U. Latif, J. Nam, A. Nelles, C. Persichilli, P. Sandstrom, J. Tatar, and E. Unger, "Observation of classically 'forbidden' electromagnetic wave propagation and implications for neutrino detection.," *Journal of Cosmology and Astroparticle Physics*, vol. 2018, no. 07, p. 055, 2018.

[31] C. Deaconu, A. G. Vieregg, S. A. Wissel, J. Bowen, S. Chipman, A. Gupta, C. Miki, R. J. Nichol, and D. Saltzberg, "Measurements and modeling of near-surface radio propagation in glacial ice and implications for neutrino experiments," *Phys. Rev. D*, vol. 98, p. 043010, Aug 2018.

[32] J A Aguilar et al, "Design and Sensitivity of the Radio Neutrino Observatory in Greenland (RNO-G)," *arXiv*, 2020.

[33] The IceCube Gen2 Collaboration, "Icecube-gen2: the window to the extreme universe," *Journal of Physics G: Nuclear and Particle Physics*, vol. 48, p. 060501, apr 2021.

[34] C. Glaser, D. García-Fernández, A. Nelles, J. Alvarez-Muñiz, S. W. Barwick, D. Z. Besson, B. A. Clark, A. Connolly, C. Deaconu, K. D. d. Vries, J. C. Hanson, B. Hokanson-Fasig, R. Lahmann, U. Latif, S. A. Kleinfelder, C. Persichilli, Y. Pan, C. Pfendner, I. Plaisier, D. Seckel, J. Torres, S. Toscano, N. v. Eijndhoven, A. Vieregg, C. Welling, T. Winchen, and S. A. Wissel, "NuRadioMC: simulating the radio emission of neutrinos from interaction to detector," *The European Physical Journal C*, vol. 80, no. 2, p. 77, 2020.

[35] S. Barwick, E. Berg, D. Besson, T. Duffin, J. Hanson, S. Klein, S. Kleinfelder, K. Ratzlaff, C. Reed, M. Roumi, T. Stezelberger, J. Tatar, J. Walker, R. Young, and L. Zou, "Design and Performance of the ARIANNA HRA-3 Neutrino Detector Systems," *IEEE Transactions on Nuclear Science*, vol. 62, no. 5, pp. 2202–2215, 2015.

[36] P. Allison, J. Auffenberg, R. Bard, J. Beatty, D. Besson, S. Böser, C. Chen, P. Chen, A. Connolly, and J. Davies, "Design and initial performance of the Askaryan Radio Array prototype EeV neutrino detector at the South Pole," *Astroparticle Physics*, vol. 35, no. 7, pp. 457–477, 2012.

[37] S. W. Barwick *et al.*, "A First Search for Cosmogenic Neutrinos with the ARIANNA Hexagonal Radio Array," *Astropart. Phys.*, vol. 70, pp. 12–26, 2015.

[38] P. Allison, S. Archambault, J. J. Beatty, M. Beheler-Amass, D. Z. Besson, M. Beydler, C. C. Chen, C. H. Chen, P. Chen, B. A. Clark, W. Clay, A. Connolly, L. Cremonesi, J. Davies, S. d. Kockere, K. D. d. Vries, C. Deaconu, M. A. DuVernois, E. Friedman, R. Gaior, J. Hanson, K. Hanson, K. D. Hoffman, B. Hokanson-Fasig, E. Hong, S. Y. Hsu,

L. Hu, J. J. Huang, M. H. Huang, K. Hughes, A. Ishihara, A. Karle, J. L. Kelley, R. Khandelwal, K. C. Kim, M. C. Kim, I. Kravchenko, K. Kurusu, H. Landsman, U. A. Latif, A. Laundrie, C. J. Li, T. C. Liu, M. Y. Lu, B. Madison, K. Mase, T. Meures, J. Nam, R. J. Nichol, G. Nir, A. Novikov, A. Nozdrina, E. Oberla, A. O'Murchadha, J. Osborn, Y. Pan, C. Pfendner, J. Roth, P. Sandstrom, D. Seckel, Y. S. Shiao, A. Shultz, D. Smith, J. Torres, J. Touart, N. v. Eijndhoven, G. S. Varner, A. G. Vieregg, M. Z. Wang, S. H. Wang, S. A. Wissel, S. Yoshida, R. Young, and A. Collaboration, "Constraints on the diffuse flux of ultrahigh energy neutrinos from four years of Askaryan Radio Array data in two stations," *Physical Review D*, vol. 102, no. 4, p. 043021, 2020.

[39] J. Hanson, "Broadband RF Phased Array Design for UHE neutrino detection," *Proceedings of 37th International Cosmic Ray Conference — PoS(ICRC2021)*, p. 1217, 2021.